DOI: 10.26650/JGEOG2024-1295793

COĞRAFYA DERGİSİ
JOURNAL OF GEOGRAPHY
2024, (48)
https://iupress.istanbul.edu.tr/en/journal/jgeography/home

Depositional Properties and Paleoclimate of a Middle-Upper Pleistocene Fan Delta Sequence in the Bor Plain, Central Anatolia, Turkey

İç Anadolu Bölgesi'nde Bor Ovası'nda Orta-Üst Pleistosen Yelpaze Delta Dizisinin Depolanma Özellikleri ve Paleoiklimi

Türkan BAYER-ALTIN[1], Zehra Semra KARAKAŞ[2], Bekir Necati ALTIN[1], Mine Sezgül KAYSERİ-ÖZER[3]

[1]Niğde Ömer Halisdemir University, Department of Geography, Niğde, Türkiye
[2]Ankara University, Department of Geological Engineering, Ankara, Türkiye
[3]Dokuz Eylül University, Institute of Marine Sciences and Technology, İzmir, Türkiye

ORCID: T.B.A. 0000-0001-8692-1713; Z.S.K. 0000-0002-5620-4518; B.N.A. 0000-0002-9570-9877; M.S.K.Ö. 0000-0003-2712-2457

ABSTRACT
The Bor Plain, which is located in the Middle Kızılırmak subregion of the Central Anatolia Region, extends 14 km toward the west of Niğde. The fan delta deposition system in the southwest of the Bor Plain was formed on the fault-controlled foothills of Mt. Keçiboyduran. The fandelta sequence shows that a paleolake formed during a phase because of the mineralogical content and frequently changing facies. Additionally, clay minerals and herbaceous plants reflecting humid and arid climatic conditions illustrate the lake-level changes. Six changes in the lake level occurred from marine isotope stage (MIS) 7 to (MIS) 5. Three major high stands occurred in the paleolake at the lowest and middle parts of the sequence. The first high stand was a stepwise transgression between ~240 and ~230 ka., and the second high stand was between ~200 and ~195 ka. The third high stand was characterized by a short transgression at 182 ka. After this stage, the lake receded significantly at 127 and 105 ka, indicating climatic control over the water level changes. In the transition from the Middle to Late Pleistocene, a revival of volcanic activity in the Leşkeri monogenic volcanic mass released volcanic material, affecting sedimentation. Volcanic rocks increase dramatically in the upper section of the fandelta during an interval that coincides with low lake-level fluctuations.
Keywords: Fan delta, Paleoclimate, MIS7

ÖZ
İç Anadolu Bölgesi'nin Orta Kızılırmak bölümünde bulunan Bor Ovası, Niğde'nin batısına doğru 14 km uzanır. Ovanın güneybatısındaki yelpaze deltası, Keçiboyduran Dağı'nın fay kontrollü eteğinde oluşmuştur. Fan delta, mineralojik içerik ve sık sık değişen fasiyes nedeniyle bir faz sırasında eski bir göl ortamında oluştuğunu göstermektedir. Ayrıca nemli ve kurak iklim koşullarını yansıtan kil mineralleri ve otsu bitkiler göl seviyesindeki değişimleri göstermektedir. Deniz izotop aşaması (MIS) 7'den (MIS) 5'e kadar göl seviyesinde altı kez değişiklik meydana geldiği anlaşılmaktadır. İstifin en alt ve orta kısımlarında eski göl ortamında üç büyük yüksek basamak meydana gelmiştir. İlk yüksek basamak, ~240 ile ~230 ka arasında ve İkinci yüksek basamak ~200 ile ~195 ka arasındadır. Üçüncü yüksek basamak 182 ka'da görülmektedir. Bu aşamadan sonra göl 127 ka ve 105 ka da önemli ölçüde gerilemiştir. Bu durum su seviyesi değişiklikleri üzerinde iklim kontrolünün olduğunu göstermektedir. Ayrıca Orta Pleyistosen'den Geç Pleyistosen'e geçişte, Leşkeri volkanik kütlesinden çıkan materyal sedimantasyona etki etmiştir. Bu nedenle volkanik kayaçlar, düşük göl seviyesi dalgalanmalarına denk gelen bir aralıkta fan deltanın üst kesiminde önemli ölçüde artar.
Anahtar kelimeler: Fan delta, Plaeoiklim, MIS7

Submitted/Başvuru: 11.05.2023 • **Revision Requested/Revizyon Talebi:** 11.12.2023 • **Last Revision Received/Son Revizyon:** 16.12.2023 • **Accepted/Kabul:** 18.12.2023 • **Online Published/Çevrimiçi Yayın:** 23.05.2024

Corresponding author/Sorumlu yazar: Türkan BAYER-ALTIN / turkanaltin@yahoo.com

Citation/Atıf: Bayer-Altın, T, Karakaş, Z.S., Altın, B.N., Kayseri-Özer, M.S.. (2024). Depositional properties and paleoclimate of a Middle-Upper Pleistocene fan delta sequence in the Bor Plain, Central Anatolia, Turkey. Cografya Dergisi. *Cografya Dergisi, 48*, 65-82. https://doi.org/10.26650/JGEOG2024-1295793

1. INTRODUCTION

Paleolake environments formed in a volcanic region, where tectonics are active, are complex systems. Often the development of such a lake is accompanied by the accumulation of fan deltas (Gruszka and Zieliński, 2021). Thus, fandeltas are crucial elements of this system. Fan deltas developing at the margins of expanded lakes provide vital evidence, recording the depositional environments and hydrological dynamics of lake basins that have experienced climatic changes in the past (Colella et al., 1992). This is reflected in the sediments forming a delta or in the morphology of the delta (Orton and Reading, 1993). The configuration of the drainage basin, the depth of the water, the transport and accumulation of sediments, and the nature of the processes in the underwater environment, which are among the main factors in the environment, affect the functioning of such a system (Rodriguez et al., 2000). The sediment load feeding the delta, which plays an important role in the shape and size of a delta, is an important aspect of facies sequences (Woronko and Pochocka-Szwarc, 2013). In addition, lake level variations are the main way in which lakes respond hydrologically, and they are significant in reconstructing past climate changes regionally and globally (Karabıyıkoğlu, 1999). In the Central Anatolian Region, paleolakes and fandeltas occupy many closed basins that developed during the glacial periods of the Quaternary (Cohen and Erol, 1969; Erol, 1991). Detailed studies about fossil shoreline deposits and associated lacustrine sediments (Kuzucuoğlu, 2019; Kuzucuoğlu et al., 2020) have provided critical data about the chronology of lake-level changes, depositional settings, and climatic conditions during the Pleistocene (Roberts, 1983). The Bor Basin is one of the closed basins developing in the southeast part of the Central Anatolia region of Turkey (Fig. 1a). The Bor Basin is surrounded by Konya and Ereğli basins to the west and volcanic mountains such as Mt. Melendiz, Mt. Keçiboyduran, and Mt. Hasan to the north (Fig. 1b, c). The closed basin corresponds to a plain that rises from 1050 to 1115 m above sea level (asl) and corresponds to the clayey–sandy bottom of an old lake (paleolake) covering an area of approximately 670 km^2. The fandelta deposition system, which is the subject of the study, is located on the fault-controlled foothills of Keçiboyduran Mountain, in the southwest of the Bor Plain. Gürel and Lermi (2008) presented the results of detailed sedimentological and partial geochemical analysis of the various non-marine sedimentary facies in the Bor Plain. Bayer-Altın et al. (2015) studied environmental and climatic changes during the Pleistocene–Holocene in the Bor Plain taking mineralogical data into account. In addition, Bayer-Altın et al. (2021) determined the relationship between the location of

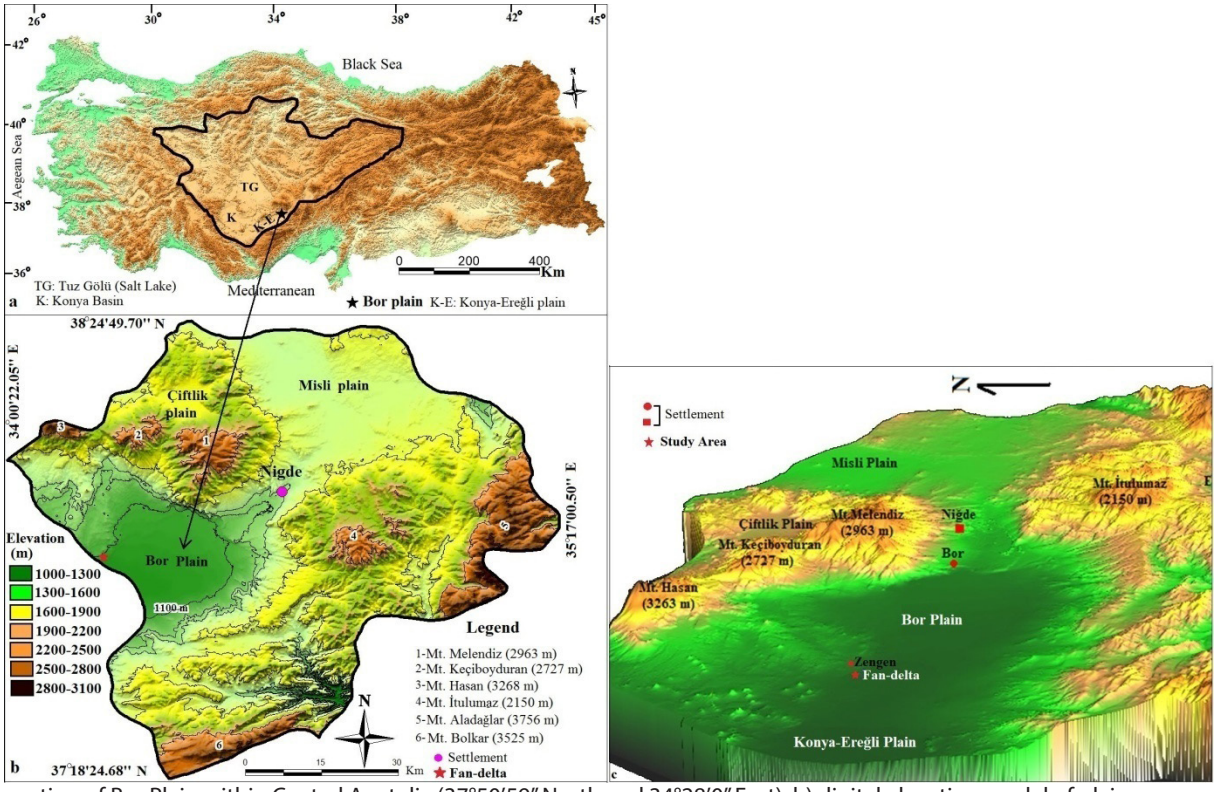

Fig. 1. a) Location of Bor Plain within Central Anatolia (37°50′59″ North and 34°28′0″ East), b) digital elevation model of plain, surroundings and location of fan delta (study area) within Niğde province (37°25′39″ North and 35°25′38″ East), c) 3D view of fan delta (37°48′46.58″ North and 34°13′51.75″ East) and location in the plain.

Neolithic sites and the lake level changes during the Holocene in the Bor Plain. However, no mineralogical, palynological, or climatological studies have been conducted on the fandelta deposition system in the Bor Plain to date.

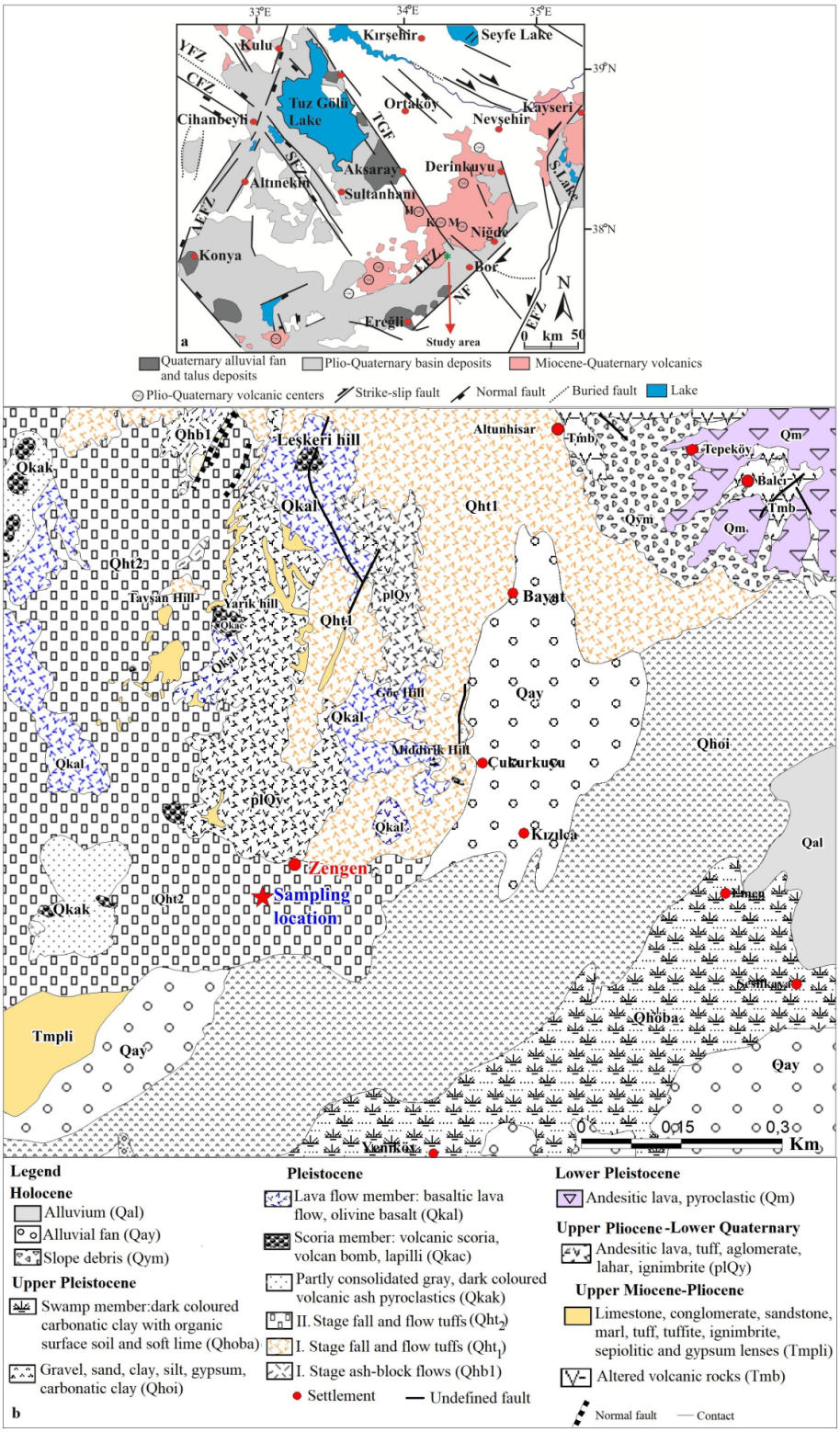

Fig. 2. a) Simplified geological map of the area surrounding the fan delta (study area) (AEFZ: Altınekin Fault Zone, YFZ: Yeniceoba Fault Zone, SFZ: Sultanhanı Fault Zone, CFZ: Cihanbeyli Fault Zone, TGF: Tuz Gölü Fault, NF: Niğde Fault, LFZ: Leşkeri Fault Zone, EFZ: Ecemiş Fault Zone, S. Lake: Sultanzaslığı Lake, H: Mt. Hasan, K: Mt. Keçiboyduran, M: Mt. Melendiz), (modified from Emre, 1991; Göncüoğlu et al., 1996), b) geological map of fan delta vicinity obtained from 1:100,000 scale geology map numbered Karaman-M32 (Ulu, 2009).

Defining the Late Quaternary history of the fandelta development and the position of adjacent streams will be the first step toward an integrated understanding of the plain and fan delta evolution over multiple climate cycles and tectonically relevant timescales. Therefore, this study will be the first comprehensive multidisciplinary study using dating techniques to contribute significantly to the understanding of the evolution of the natural environment of the Bor Plain under the influence of past climate changes. This study aims to evaluate the spatial-temporal relationships of the depositional environments in the fandelta succession in the plain, to consider regional volcanic activities, and to evaluate the glacial/interglacial depositional history of the plain.

2. Geological Setting

The fandelta and its surroundings, which are the subject of the study, are located in the Bor Plain. The plain is located in the southeastern part of the Central Anatolian Region of Turkey. The area is at the intersection of many active fault zones (Fig. 2a).

Much volcanic activity occurred from the Miocene to Holocene depending on these zones. Miocene-Holocene volcanic activity occurred in the Bor Plain, differing in the type, products, and age of volcanism. Large volcanic complexes, large ignimbrite outcrops, and numerous monogenic volcanic structures formed in the region (Agostini et al., 2015). The Upper Miocene-Pliocene volcanics and volcaniclastics of the Melendiz Group located in the north of the study area cover extensive areas (Atabey et al., 1990). A recent study (Doğan-Kulahçı et al., 2018) dated the volcanism of Obruk-Zengen (i.e. Leşkeri Hill) samples to between 0.6 and 0.2 Ma ($^{40}Ar/^{39}Ar$). The dominant fault is the Leşkeri Fault (LF) which has affected the development of the Bor Plain, and volcanism at the edge of the plain (Emre, 1991). Basalts emerged from centers aligned with N-S trending volcanic cones due to this opening fissure. The LF was defined as an opening fissure by Emre (1991). Many Lower Quaternary basaltic volcanic cones lie along the fault zone north of the fandelta. Basalts emerged from centers aligned with N-S trending volcanic cones due to this opening fissure (Fig. 2b).

3. MATERIAL AND METHODS

Sand samples were collected in 2018 and 2019 from a sand quarry positioned in the lowest part of the Bor Plain c. 5 km from the village of Zengen. The sand quarry consists of lake sediments with approximately 30 m thickness. The coordinates of the sampling site are 37°48'47.34" north and 34°13'47.26" east. Samples were analyzed with (1) thin-section petrography; (2) mineralogy determined by powder X-ray diffraction (XRD); (3) optically stimulated luminescence (OSL) dating; (4) organic carbon content; (5) calcium carbonate content, and (6) fossil pollen analysis.

In the field, samples were taken from a fandelta that developed in front of the Late Pleistocene volcanic flow tuffs moving towards the Bor paleolake, which represents a sand quarry sequence. Fourteen samples were collected from horizons with different lithologies. Thin sections were prepared from hard and cemented samples, and then the mineralogical compositions and textural properties of these samples were examined under a polarizing microscope (Leica; DM/LSP). The mineral composition of the samples was determined by powder XRD at the Central Laboratory of Niğde University using a Panalytical diffractometer. The XRD analyses were performed using Cu-*Kα* radiation with a scanning speed of 0.02°2θ/min. Samples were prepared for clay mineral analyses (size fraction<2 μm) by separating the clay fraction by sedimentation, followed by centrifugation of the suspension after overnight dispersion in

Table 1. Results of luminescence dating of samples from the fan delta in the Bor Plain

Sample code	Depth (m)	g value	Used Aliq.	Grain size (μm)	Eq. dose (Gy)	U (ppm)	Th (ppm)	K (%)	Water (%)	Cosmic dose rate ($Gy.ka^{-1}$)	External dose rate ($Ga.ka^{-1}$)	Internal dose rate ($Gy.ka^{-1}$)	Annual dose rate ($Gy.ka^{-1}$)	Fading corrected age (ka)
L1	28.0	4.9±0.6	16/16	90-125	438±60	3.33±0.13	17.27±0.69	1.42 ± 0.06	30±5	0.03±0.01	2.73±0.11	0.04±0.01	2.77±0.11	230 ±35
L1a	27.5	1.4±0.2	16/16	90-125	356±40	1.84±0.07	8.6 ± 0.34	0.99 ± 0.04	30±5	0.03±0.01	1.61±0.06	0.03±0.01	1.64±0.06	240 ±27
L1b	27.0	1.6±0.2	16/16	90-125	509±47	2.88±0.12	15.91±0.64	1.17 ± 0.05	30±5	0.03±0.01	2.38±0.1	0.04±0.01	2.42±0.1	233 ±24
L2	25.0	1.1±0.2	16/16	90-125	551±49	3.23±0.13	13.63±0.55	1.06 ± 0.04	30±5	0.03±0.01	2.24±0.09	0.03±0.01	2.27±0.09	261 ±28
L3	20.0	1.8±0.2	16/16	90-125	401±26	2.86±0.11	14.9 ±0.6	1.3 ± 0.05	30±5	0.04±0.01	2.43±0.1	0.04±0.01	2.47±0.1	182 ±14
L4	15.0	1.5±0.2	16/16	90-125	378±19	3.35±0.13	22.34±0.89	1.64 ± 0.07	30±5	0.06±0.01	3.23±0.13	0.05±0.01	3.27±0.13	127 ±14
L5	12.0	1.4±0.2	16/16	90-125	220±37	4.24±0.17	11.12±0.44	0.97 ± 0.04	30±5	0.07±0.01	2.27±0.09	0.03±0.01	2.3±0.09	105 ±15
L6	10.0	1.6±0.2	16/16	90-125	468±58	3.32±0.13	14.88±0.6	1.28 ± 0.05	30±5	0.09±0.01	2.55±0.1	0.04±0.01	2.58±0.1	200 ±27
L7	8.0	1±0.1	16/16	90-125	389±39	2.25±0.09	10.66±0.43	1.25 ± 0.05	30±5	0.1±0.01	2.09±0.08	0.04±0.01	2.12±0.08	195 ±30
L8	5.0	1.4±0.2	16/16	90-125	409±42	1.71±0.07	5.94 ±0.24	0.95 ± 0.04	30±5	0.14±0.01	1.52±0.06	0.03±0.01	1.55±0.06	289 ±35
L9	3.0	1.5±0.2	16/16	90-125	368±37	2.4±0.1	9.59 ±0.38	1.01 ± 0.04	30±5	0.18±0.02	1.94±0.07	0.03±0.01	1.97±0.07	205 ±28
L10	2.0	1.5±0.2	16/16	90-125	396±43	2.33±0.09	10.44±0.42	1.07 ± 0.04	30±5	0.2±0.02	2.06±0.08	0.03±0.01	2.09±0.08	210 ±25
L11	1.0	2.6±0.3	16/16	90-125	368±31	1.91±0.08	9.96 ±0.4	1.05 ± 0.04	30±5	0.23±0.02	1.95±0.07	0.03±0.01	1.98±0.07	222 ±24
L12	0.6	1.8±0.2	16/16	90-125	377±26	2.29±0.09	7.04 ±0.28	0.9 ± 0.04	30±5	0.25±0.03	1.77±0.07	0.03±0.01	1.8± 0.07	236 ±18

distilled water (Moore and Reynolds, 1997). Luminescence analyses of collected samples were conducted at the Luminescence Research and Archeometry Laboratory of Ankara University, Institute of Nuclear Sciences, Turkey. Samples taken for OSL analysis were crushed and powdered in a mortar, and grains of 90-180 μm were separated under weakened red light in the laboratory. The samples were analyzed using appropriate chemicals (for example, grains were treated with 10% HCl and 10% $H2O_2$ for the removal of carbonates and organics, respectively) adhering to the principles of the feldspar pIRIR technique age determination. Luminescence dating analysis results of all samples whose ages were calculated are given in Table 1. The total organic carbon (TOC) content of 14 samples obtained from the fandelta was also estimated by the titration method described by Gaudette et al. (1974). The amount of organic carbon in the solid matter was measured as a percentage.

The $CaCO_3$ amount in the samples was measured under laboratory conditions with a Schiebler-type calcimeter. Temperature and pressure corrections were considered when calculating the measured value. This measurement is performed by measuring the pressure of CO_2 gas produced from the reaction of samples with hydrochloric acid (HCl). The samples were studied for pollen analysis under a microscope using standard palynological techniques for disintegrating Quaternary sediments, which includes successive treatment with hydrochloric acid (HCl), hydrofluoric acid (HF), potassium hydroxide (KOH), and heavy liquid separation ($ZnCl_2$). Samples were stored in glycerin. A minimum of 150 pollen grains from terrestrial plants was counted in each sample. The identification of poromoprhs was performed at the lowest possible taxonomic level by comparing fossils with their current relatives in pollen atlases and the keys of some researchers (Beug, 2004).

4. RESULTS

4.1. Facies analysis

The Middle-Late Pleistocene fandelta units in the sand quarry are divided into 7 lithofacies according to their lithology, textural

Table 2. Lithofacies description and environmental interpretation of Middle-Upper Pleistocene deposits in the Bor Plain.

Facies	Description	Interpretation
F1- Cross bedded, clast supported cream-beige sandstone	Matrix free sand, medium to fine-grained size, cream-beige colour, cross bedded (40-50 cm thick), erosional surface	Stream-delta deposits (Smith, 1986; De Celles et al., 1991)
F2- Cross bedded, black gravelly sandstone	Matrix free coarse sand fine pebbles (30-40%), black moderately sorted and rounded, coloured,manganese plastering, 40 to 50 cm thick cross bedded (total 4-5 m).	Delta deposit (Rust, 1978; Karabıyıkoğlu, 2003)
F3- Matrix supported gravelly sandstone	Beige-yellow-gray coloured, unsorted, 50-100 cm thick beds composed of fine pebbles and coarse sand, carbonate matrix supported.	Lakeshore (Horton and Schmitt, 1996)
F4- Sandy limestone	Dark yellow, 75-100 cm thick beds composed of medium-coarse-size sand (10%), carbonate cement	Carbonate-saturated shallow and stagnant lake-stream deposits (Hardie et al., 1978; Varol et al., 2016; Akıska and Varol, 2020)
F5- Parallel bedded sandstone	Dark gray-yellow-beige coloured, matrix free, fine-to-medium grained sand, moderately to well-sorted, normal grading, 40-50 cm thick.	Flood plain deposits (Rust, 1978)
F6- Volcanic gravelly sandstone	Cream-beige moderately sorted and rounded, 40-50 cm thick beds composed of medium to coarse volcanic pebbles and fine sand, carbonate matrix supported	Flooding (Smith, 1986)
F7- Sandy rhizolith	Beige to cream calcarenite, micritic and sparitic, travertine appearance, tubular structure, overlying F6.	Carbonate sedimentation and freshwater conditions in warm shallow lake (Alçiçek et al., 2007; Akıska and Varol, 2020).

features, grain shape, cement material, and sedimentary structure (Table 2). In this section, both the analysis results and evaluations are given in the order of depositional sequence from bottom to top (Fig. 3).

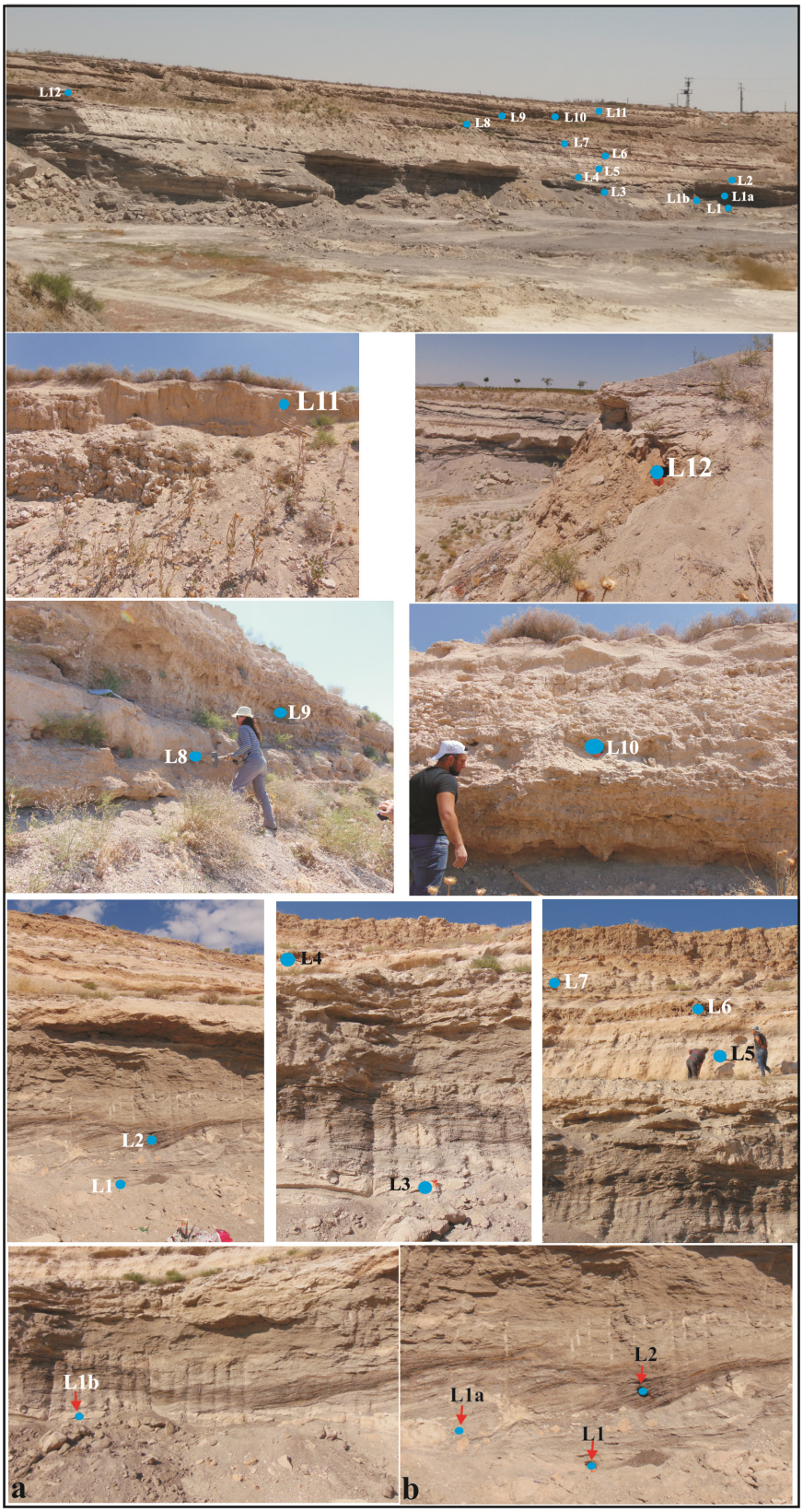

Fig. 3. Location of samples in the fan delta system (coded L1, L2, etc.) between 37°48′46.58″ North and 34°13′51.75″ East. The section is about 30 m long. The blue circle shows sample locations for OSL dating. Photos (a, b) show cross-bedding in sandstone beds.

Lithofacies F1-cross-bedded, clast supported, light yellowish grey sandstone, Description: Lithofacies is represented by very light yellowish grey sandstone (sample L1), and stratigraphically forms the base of the depositional sequence (Fig. 4). The sandstones are moderate to well-sorted. Scattered gravel clasts are sub-angular to well-rounded, derived from sandstone (sample L1a) and sandy limestone (sample L1b). L1a and L1b are composed of quartz, plagioclase, and hornblende minerals and rock fragments. Rock fragments were generally observed as rocks with a volcanic origin, which can be defined as basalt and andesite (Fig. 5). These facies have an erosional base, and cross strata sets are 15-30 cm thick. It has a thickness of 40 m to 50 cm and is overlain by cross-bedded, black pebbly sandstone of the lithofacies F2.

Interpretation: Cross-bedding, which indicates rapid sedimentation, is fed by multiple sources, and the feed direction changes from time to time beds characteristically develop overlapping each other in the facies. Cross-stratified sand and gravel deposits indicate that beach-shoreface sediments were deposited by high-energy streams, representing a progradation episode in the fandelta deposition.

Lithofacies F2 -cross-bedded, black gravelly sandstone, Description: Lithofacies F2 (sample L2) consists of black, moderately to well-sorted, cross-stratified sandstone with rounded granules and medium pebbles with manganese coating. The thickness of the cross-strata sets is 50–100 cm. Units have erosional bases and are up to 4-5 m in thickness but can be followed laterally over only a few meters due to outcrop limits. *Interpretation:* The cross-bedded sandstone with manganese-coated, gravelly sandstone units was deposited as the delta facies of a river system entering the lake. Generally, manganese coating develops on gravel and infiltrates the gravel (Tekin et al., 2005).

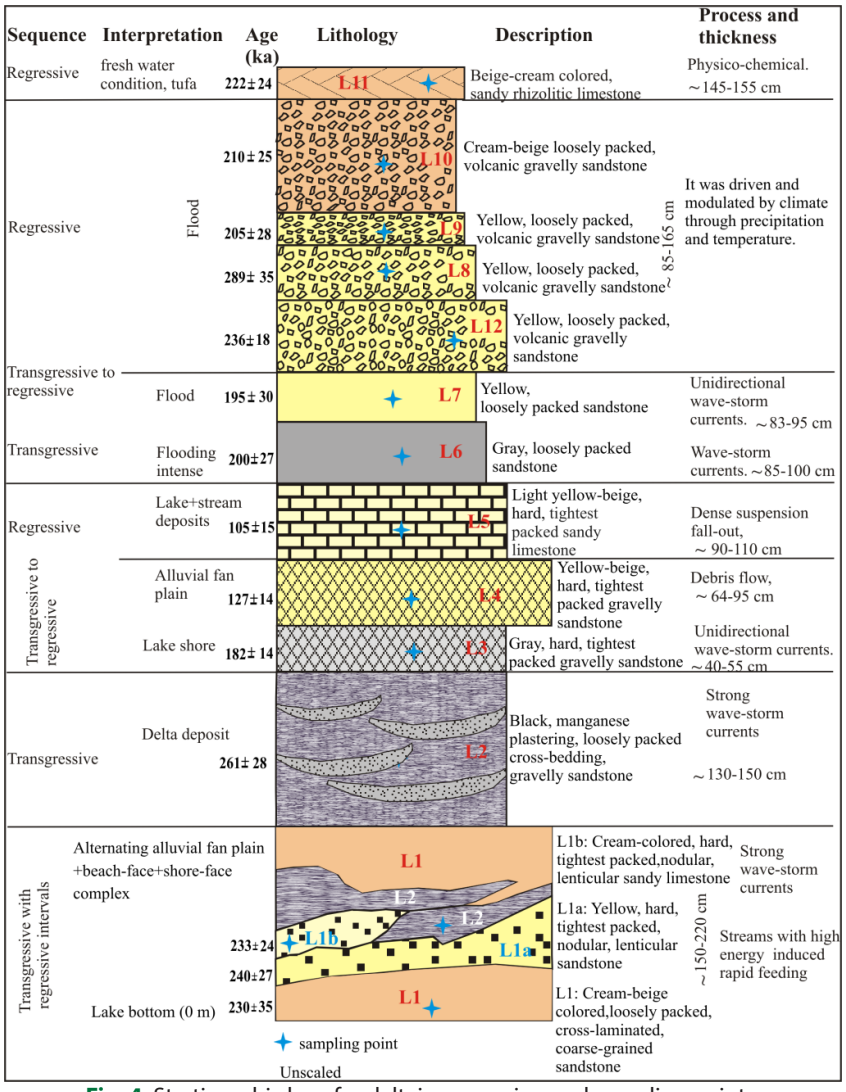

Fig. 4. Stratigraphic logs for deltaic succession and sampling points.

Beekman (1966) suggested that there was a long solfatara phase based on manganese sediments and silicified zones in the pyroclastic materials of Mt. Keçiboyduran volcanic/pyroclastic rocks. The age of the volcano is Lower Pliocene. This shows that the manganese series, which are mixed at lower levels in the fandelta, may have been transferred from here.

Lithofacies F3 -matrix-supported gravelly sandstone, Description: This lithofacies consists of well-indurated, matrix-supported pebbly sandstone (samples L3 and L4) with different thicknesses and colors such as gray, yellow, light yellow, and beige. The matrix comprises carbonate micrite and sparite. The grain components of L3 are composed of quartz, feldspar, and volcanic rock fragments, and are bonded by a matrix consisting of sparite and sparicalcite (Fig. 5). *Interpretation:* The cementing of the gravelly sandstones to each other by a matrix indicates the presence of chemicals such as carbonate in the depositional environment, and that deposition was slow. The gravelly sandstone facies were deposited on the lake shore. *Lithofacies F4 -sandy limestone, Description:* This lithofacies is represented by dark yellow (sample L5) sandy limestone, is about 75-100 cm in thickness, and consists of coarse- to medium-grained sand (10%). The matrix comprises carbonate micrite and sparite. Volcanic rock fragments are cemented with a micrite and microsparite matrix (Fig. 5). L5 was identified as lithic wacke. These sandy limestones have lateral extent, overlying the sandstone lithosome of lithofacies F5. *Interpretation:* This sandy limestone lithofacies indicates an increase in lake water depth, perhaps due to subsidence of the graben floor (Ilgar and Nemec, 2005), accompanied by a greater influx of terrigenous sand from the lake margins, probably due to rain wash and wave action (Hardie et al., 1978). The sedimentation rate increased, and the lake level continued to fluctuate, but episodes of emergence were shorter and less frequent (Akıska and Varol, 2020). *Lithofacies F5 - parallel-bedded sandy limestone, Description:* This lithofacies consists of several alternations of grey, yellow, and beige-colored loosely-packed sandstone (samples L6 and L7) with different thicknesses (40-50 cm) and containing lateral lenses. Lithofacies F5 is represented by sandy limestone and is moderate to well-sorted. In the L7 sandstone sample, the grain components of the unit are composed of quartz, plagioclase, and rock fragments (Fig. 5). The cement is sparite, less than 15%, and the rock is called lithic arenite. The lithofacies rest on the sandy limestone of lithofacies F4 and underlies the volcanic gravelly sandstone of lithofacies F6. *Interpretation:* The loose-packed state and the wedging of the sandstone indicate a rapid flow and flooding period in the underwater environment. It also shows that these incidents occurred under fault control. This lithofacies is represented by a river deposition system where flooding is intense. *Lithofacies F6 -volcanic gravelly sandstone, Description:* This lithofacies consists of alternating gravelly sandstone (samples L12, L8, L9, and L10) with different colors and thicknesses. In addition, there are volcanic gravels of different sizes in the sandstone. This indicates that the depositional environment was fed by units with volcanic origin. In the L8 volcanic gravelly sandstone sample, plagioclase, calcite, quartz, cristobalite, pyroxene, mica minerals, and volcanic pebbles were determined by the petrographic investigation (Fig. 5). The volcanic gravels in L10 are called basalt, similar to samples L8 and L9 (Fig. 6). These gravels in the sandstone must be products of intermediate-basic volcanism with Upper Miocene-Pliocene and Holocene age in the region. *Interpretation:* Gravelly sandstones formed as a result of the deposition of pebble-sized volcanic material and sand-sized siliciclastic material brought to the environment during periods of chemical precipitation and flooding. The presence of cement such as sparite and sparicalcite in the sandstone, amounting to between 10% and 15%, also indicates the presence of carbonate material and chemical precipitation in the environment. *Facies F7- sandy rhizolithic limestone, Description:* This lithofacies consists of beige-cream limestone (sample L11) and stratigraphically forms the upper section of the depositional sequence. It is observed as volcanic gravel, sand, and clay when examined considering lithological features vertically and laterally. The level of this sandy limestone lithology also has a morphologically different appearance in the field. The L11 sample is a sandy rhizolithic limestone unit composed of quartz with micrite and sparite cement (Fig. 6). These limestones are represented by laminations and travertine appearance. This is created by the accumulation of minerals around plant roots or internal precipitation as cement, and replacement. *Interpretation:* The rhizolith limestones indicate a shallow carbonate lake (Cramer and Hawkins, 2009).

4.2. Geomorphology of the fandelta area

An old alluvial fan system developed in front of Kule Stream Basin (Basin 1) (Fig. 7a). The drainage system of Basin 1, extending to the volcanic cone of Leşkeri Hill (1522 m) located about 19 km north of the study area, played an important role in the formation of the old alluvial fan. West of the basin is the volcanic cone of Yarık Hill (1356m). These cones are located on lava and pyroclastics of an older southward volcanic flow. Considering the drainage network, the Yarık cone appeared later than the Leşkeri cone. Considering the other individual cones (Göç and Middirik hills) and Kartalkaya Ridge located to the

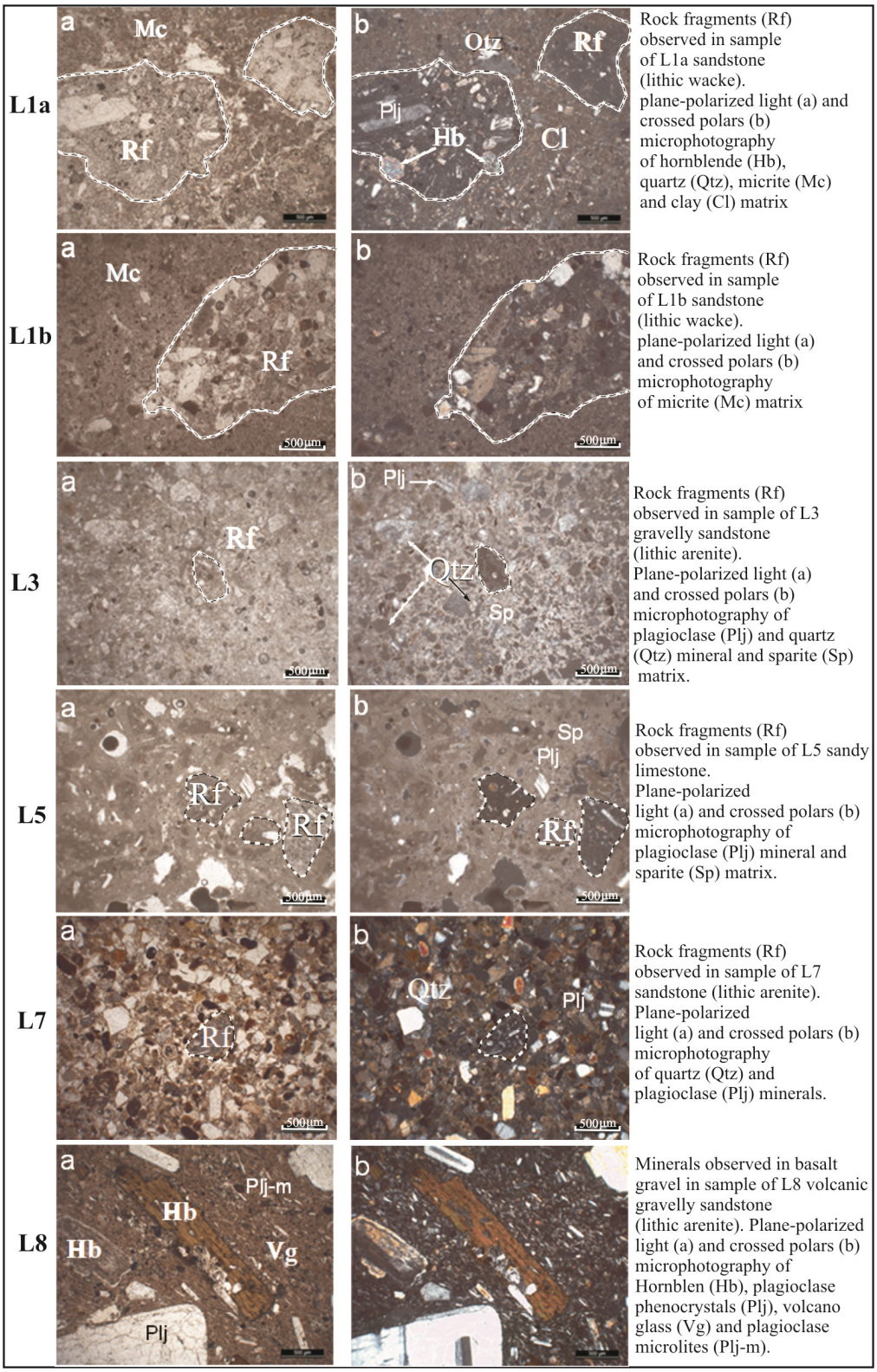

Fig. 5. Thin section photomicrographs of sandstone samples L1a, L1b, L3, L5, L7, and L8.

east of the basin, the drainage of Basin 1 developed between these cones in the Pleistocene. The approximate elevation difference between the location where the samples were taken, and the bottom of the plain is 285 m.

With the lava and pyroclastics extending to the south along 5% and 10% slopes, the erosional-accumulation surfaces exposed in places are cut by faults at 1100 m (asl). Basin 2 (Devetaşı Stream Basin) is a young drainage system developing

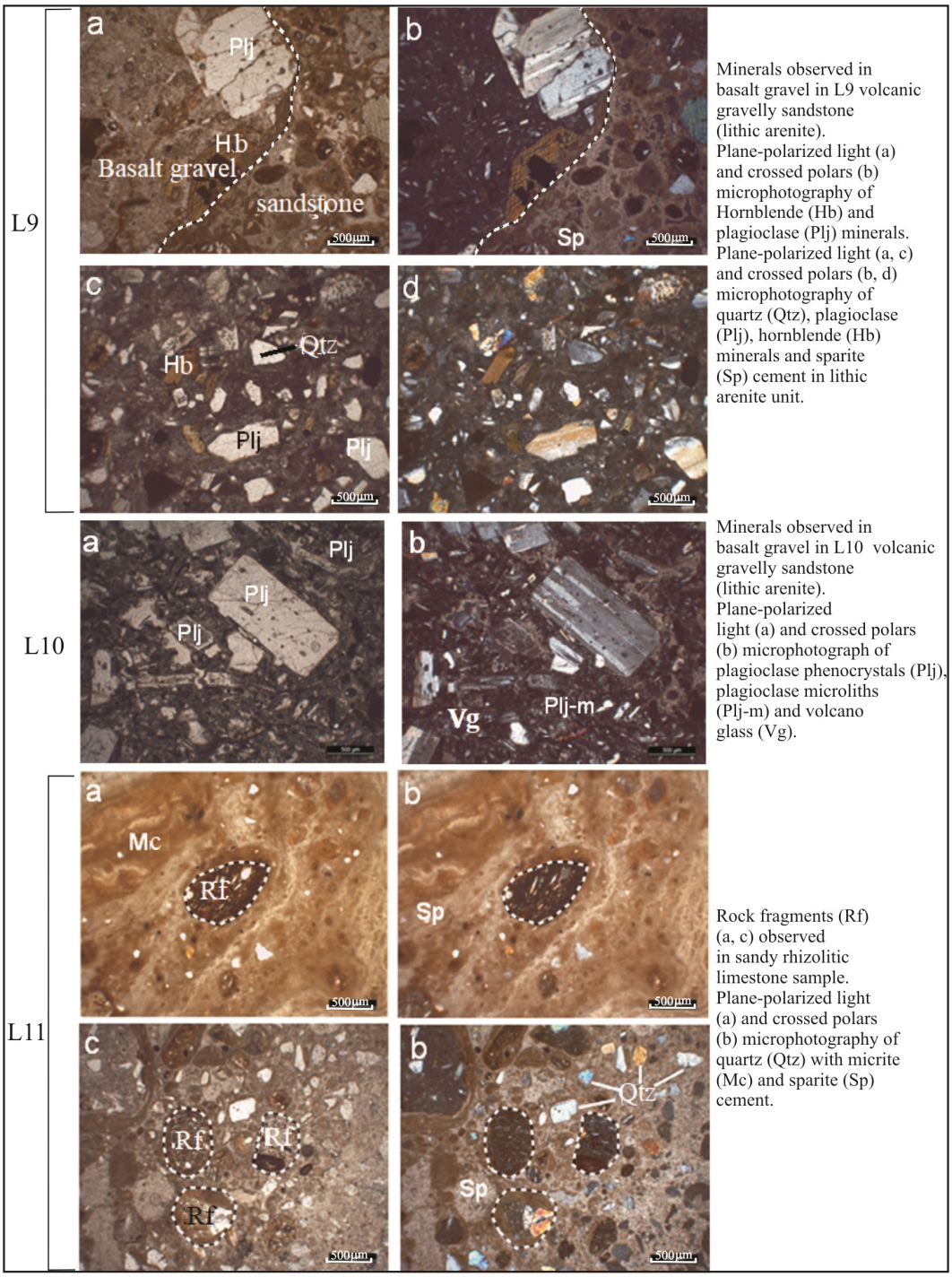

Fig. 6. Thin section photomicrographs of sandstone samples L9, L10, and L11.

backward in front of sedimentary and volcaniclastics after the emergence of basaltic strombolian cones. Therefore, it forms the western edge of the alluvial fan that reached Zengen in the past. The streams of Basin 2 later eroded the fan, including old and new materials in lenses within the depositional sequence (Fig. 7a). Following rainy periods, the streams deformed the old fan and its cones. Simultaneously, riverbanks formed between the cones, and the streams settled between the existing deposits, causing the stratigraphic sequence to become more complex. While limestones occurred in phases when freshwater input was the most intense in the lacustrine area, they formed thick deposits during phases when heat and evaporation were high. Alluvial-colluvial material and old transported material with a glacis (sloping foothill level formed by surface flow flood waters and colluvial soil movements resulting from the effects of periodic rainy and dry seasons) character, which consist of complex

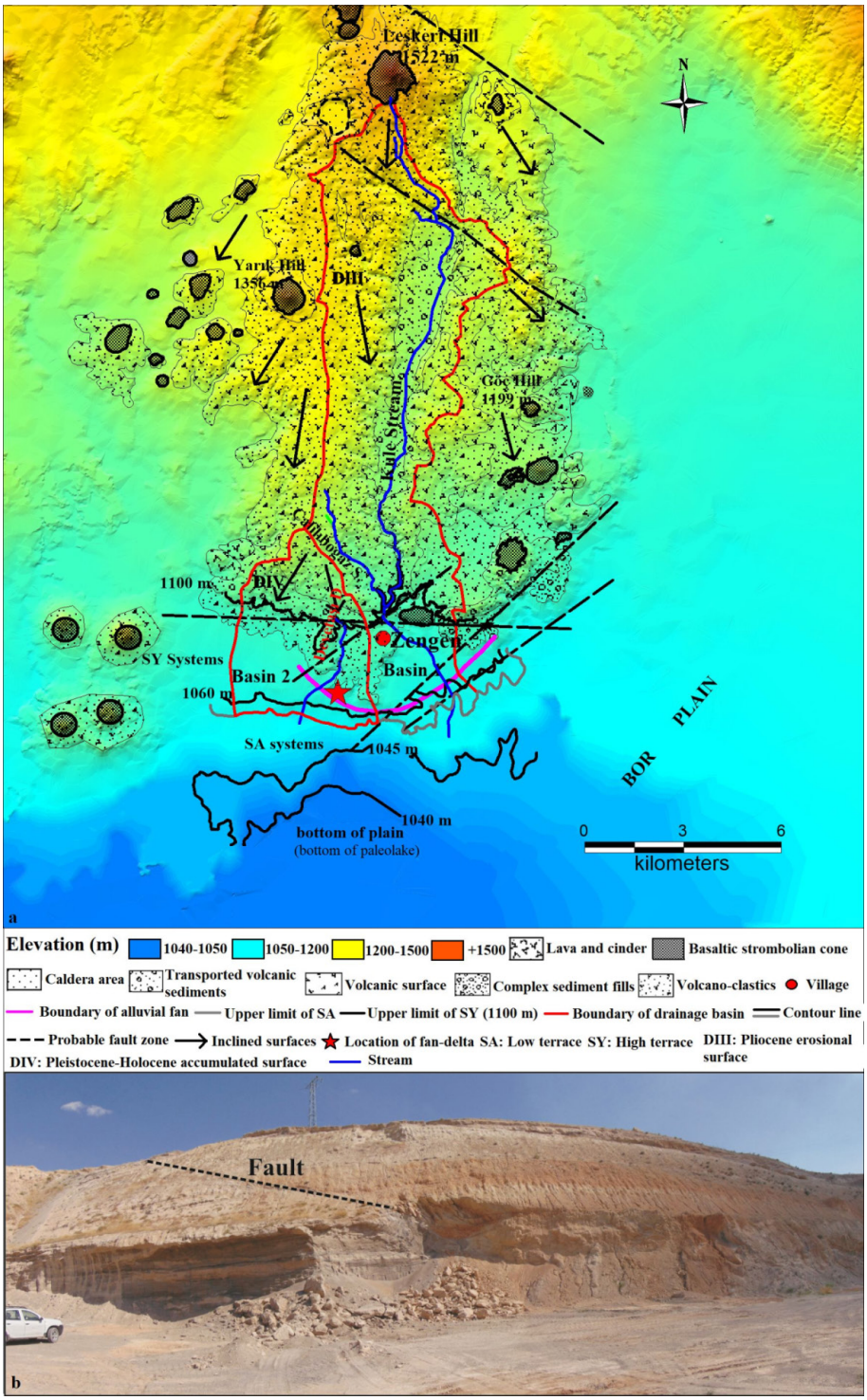

Fig. 7. a) Simplified geomorphology map of the study area (Zengen village and environs where fan delta is located) and surroundings, b) one of the strike-slip faults in sandstone unit viewed from north to south. It also shows that sedimentation occurred under fault control. The location is between 37°48′44.84″ North and 34°13′50.68″ East.

materials carried and accumulated by flooding streams on the surface extending from the mountainous area to the Bor Plain, are distributed over a wide fan area from the mouth of the Kule Stream Basin. The glacis surfaces formed different layers from the Lower Pleistocene to the Holocene with a lateral transition from lacustrine sediments consisting of finer element material towards the plain floor at lower levels. Thus, the fan delta received significant direct input of sediment including gravels transported by runoff and intermittent streams from the volcanic terrain immediately adjacent to the lake. Twelve distinct facies

representing both subaerial and subaqueous depositional processes are preserved within the fan delta depositional sequence system. In Figure 7, the bottom of the plain corresponds to the paleolake. This system consists of material transported towards the paleolake and includes cross-bedding. Cross-bedding observed in the fan delta reflects different streamflow and climatic periods. In addition, many layers were inclined in the fan delta, which is faulted in places; thus, the transition between layers cannot be followed (Fig. 7b). In this study, faults seen in the fan area were also evaluated as being from a younger generation. The NW-SE trending fault passing north of Leşkeri Hill must have occurred after lava flowed from Mt. Keçiboyduran because the lava flows were cut in front of the fault and volcanic outlets which caused a new volcanic spreading surface. Since the NW-SE trending fault that passes south of Leşkeri Hill occurred after the emergence of the hill, the lava flows formed a steep slope towards the plain. In the southern part, there is a west-trending fault at 1100 m elevation. In the southern part, the high terrace (SY) systems formed as a result of Late Pleistocene subsidence due to the tectonics affecting the Bor Plain. SW-trending faults extending to the south also form young tectonic lines by the Niğde Fault. These faults also caused old lacustrine level changes and the formation of stepped-level plains consisting of stream sedimentary deposits in the front part of the low terrace (SA) systems. The level of 1040 m corresponds to the lowest level of the Bor Plain stream system. This level, which reveals itself at about 1040 to 1050 m on the contour elevation curve, has a complete sandy silty cover layer on the surface. However, the backward extent of the level appears to form lacustrine levels, which also contain stream materials mixed with debris at the edges of low hilly or old volcanic remains. The level of 1060 m (asl) corresponds to the old fan field and the terrace systems found among the glacis (DIV system), which spreads up to 1100 m in the area (Fig. 7a).

4.3. Mineralogical determination by X-ray Diffraction, $CaCO_3$, and total organic carbon (TOC)

The mineralogical results for X-ray diffraction analyses of the samples collected from the fan delta deposits are presented in Figure 8a. The assemblage of clastic minerals contains augite (pyroxene group), plagioclase, calcite, mica and cristobalite. K-feldspar, hornblende, goethite, and quartz are present in trace amounts and comprise less than 10%. Also, this mineral paragenesis is not uniform in the vertical and horizontal directions, which display different proportional alternations. Augite varies between 11% and 55% in all parts of the sequence. Its maximum value is reached in L12 (50%) and L5 (55%). Augite is followed by plagioclase, with a value varying from 4% to 48%. The maximum proportion of mica occurs in L6 (23%) and L4 (25%). It reaches a minimum value (10%) in the lower part (L1, L1a and L1b). Calcite is a trace mineral in L1, L1a, L3, L6, L10, and L11, forming less than 10%. Calcite values reach their maximum rates of 19% and 20% in L1b and L5, respectively. Its value varies from 10% to 16% in other levels. K-feldspar is above 10% in L3 (12%) and L6 (12%). Phillipsite is found in the L9, L10, and L11 levels and rises above 20%. The different clay minerals identified in the fan delta include illite, chlorite, kaolinite, smectite, palygorskite, and mixed layer (illite-smectite) clay minerals (Fig. 8b). Illite is the most dominant clay mineral in all parts of the core. It comprises about 37% of the total clay mineral assemblage. Illite varies between 35% and 40% in all parts of the sequence. Its maximum and minimum values are reached in L1 (40%) and L7 (35%), respectively. Illite comprises

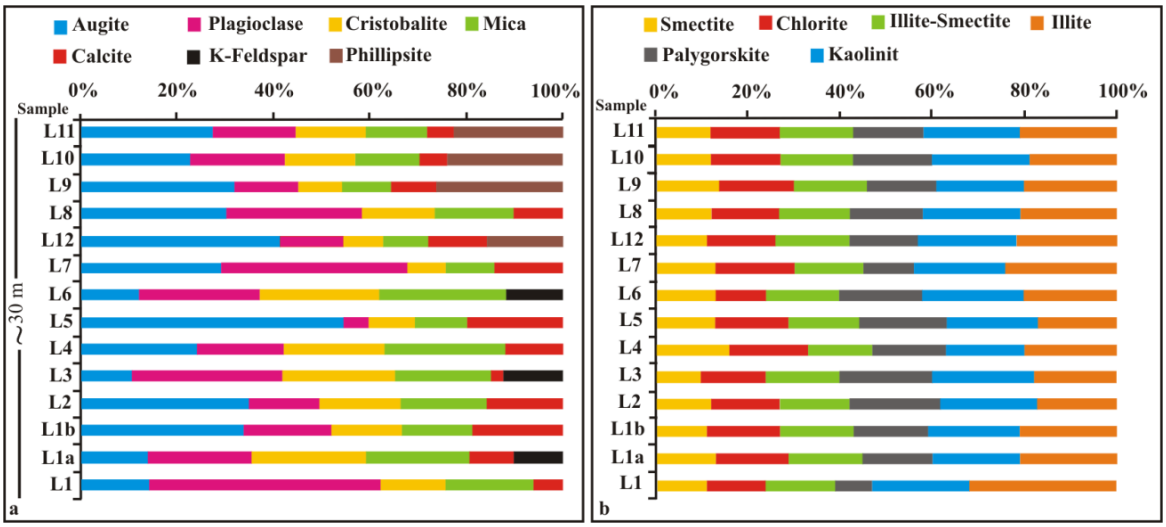

Fig. 8. Vertical change in percentage detritus (a) and clay minerals (b) content of fan delta deposits (see Fig. 4 for the legend of stratigraphy).

38% of L3, L6 and L12. Illite is followed by kaolinite with values varying from 17% to 22%. The maximum value of kaolinite is reached in L6 and L3 at 22%. The rate of kaolinite declines below 20% in L4 and varies between 19% and 21% in other levels. Palygorskite varies between 8% and 20% in all parts of the sequence.

Figure 9c shows the $CaCO_3$ and TOC ratios. $CaCO_3$ in the fan delta sediments reflects contributions from carbonate (calcite and limestone) grains, and its value varies between 2% and 54% in all parts of the core. The maximum value of $CaCO_3$ is attained in L5 and L12 (54%). The $CaCO_3$ rate decreases below 4% in L3 and L6 and varies between 11% and 42% in other levels. Evident increases in calcite concentrations are detected in L5 and L12, corresponding to approximately 105 and 236 ka, respectively. The TOC content varies between 0.17% and 0.73% (average 0.42%) and shows a variation pattern similar to the carbonate content. Organic carbon values are higher than the average value (0.42%) in L1, L1a, and L1b. Its value is close to the average from L3 to L12 and reached the lowest value (17%) in L8. Smaller amplitude increases in TOC values were also detected within L9, L10, and L11.

4.4. Palynoflora

The samples of the L1 (230±35ka; MIS 7d), L1a (240±27ka; MIS 7e), L1b (233±24 ka; MIS 7d), L2 (261±28 ka; MIS 8b), L3 (182±14 ka; MIS6e), L4 (127±14 ka; MIS 5e), L5 (105±15 ka; MIS 5c), L6 (200±27 ka; MIS7a), L8 (289±35ka; MIS 9a), L9 (205±28 ka; MIS7b), L10 (210±25 ka; MIS 7c), and L11 (222±24 ka; MIS 7d) were studied for the recoding palynofloral data (see Table 2). However, these samples cannot contain palynomorphs. This absence could be related to coarse clastic lithofacies due to the fluvial deposition system and/or effective volcanic activity in the Bor Plain. Fossil pollen was detected in two samples, L7 and L12. Palynoflora in the L7 sample (195±30 ka; MIS7a) is only represented by more abundant Chenopodiaceae, Amaranthaceae, *Daphne,* and Ranunculaceae-*Thalictrum* and also lower percentages of Asteraceae-Asteroideae type. Microflora in the L12 sample, characterized by volcanoclastic sediments (236±18 ka; the boundary of the MIS 7e- 7d) which is located just above the L7 sample, contains a high percentage of Asteraceae-Asteroideae type and Ranunculaceae-*Thalictrum* among herbaceous plants. Especially, the L7 and L12 sample levels of the sedimentary sequence contain an absence of arboreal pollen and a high abundance of these herbaceous pollen species which could be explained as due to this volcanic event causing a reduction in the variety of paleovegetation.

5. DISCUSSION

5.1. Evaluation of clay and detrital minerals in terms of climate change

The fan delta deposition system is on the fault-controlled foothill of Mt. Keçiboyduran, bordering the southwest of the Bor Plain. Many Lower Quaternary basaltic volcanic cones lie along the fault zone north of the fan delta. The faults reactivated by volcanic activity and geomorphological development caused volcanic sand and gravel material to be included in the sequence during the deposition of the fan delta. The clay and detrital mineral type and abundance ratio were controlled by source rock lithology and climate in the fan delta sequence (Fig. 9a, c). For this reason, paleoclimate and paleoenvironmental evaluation of samples is associated with the prevailing climate process. The association of clay minerals such as smectite – kaolinite – chlorite – illite indicates that they come from both mafic and felsic sources and are affected by physical erosion and chemical weathering processes (Hadji et al., 2019). Levels (L1, L1a, b, L3, L6) where the amount of illite increases in the sequence indicate conditions where cold, dry physical decomposition was high, evaporation was low, and the lake level was high (Fig. 9a). illite mainly forms as a result of the physical decomposition of crystalline basic rocks rich in felsic silicates in dry climates (Weaver, 1989). Cross-bedding and detritus containing illite indicate that physical weathering was strong and streams with a high flow rate caused rapid feeding due to lack of evaporation (Fig. 9b). In the fan delta, the chlorite content is high in the transition from level L1 to levels L3 and L4 (Fig. 9a). In this study, the low amount of plagioclase in the lower levels of the fan delta was related to strong physical weathering (Fig. 9c). The plagioclase composition in river sediments is controlled by chemical decomposition (Nesbitt et al., 1996). According to Grant (1963), plagioclase is included in the environment when source rock containing feldspar is exposed to chemical decomposition. L1 level developed under cold and dry climatic conditions. Level L2 where the amount of smectite increases indicates conditions that were hot and humid, chemical decomposition was high, evaporation was high, and the lake level was low (Fig. 9a). Smectite forms as a result of the decomposition of volcanic rocks by hydrolysis, mostly in temperate and semi-arid regions (Weaver, 1989). Calcite was transported to the environment in cold periods by streams with increased flow rates and began to precipitate in hot periods. Calcite and total clay (Tclay) values show opposite proportions at all levels. Tclay was transported to the lake by streams during cold periods when there was strong physical weathering and thus

deposited in periods when the lake level increased. Augite (pyroxene group) is characteristic of some volcanic rocks such as rhyolite, andesite, and basalt, and is considered a regular detrital mineral in sediment (Boggs, 2009). A high percentage of

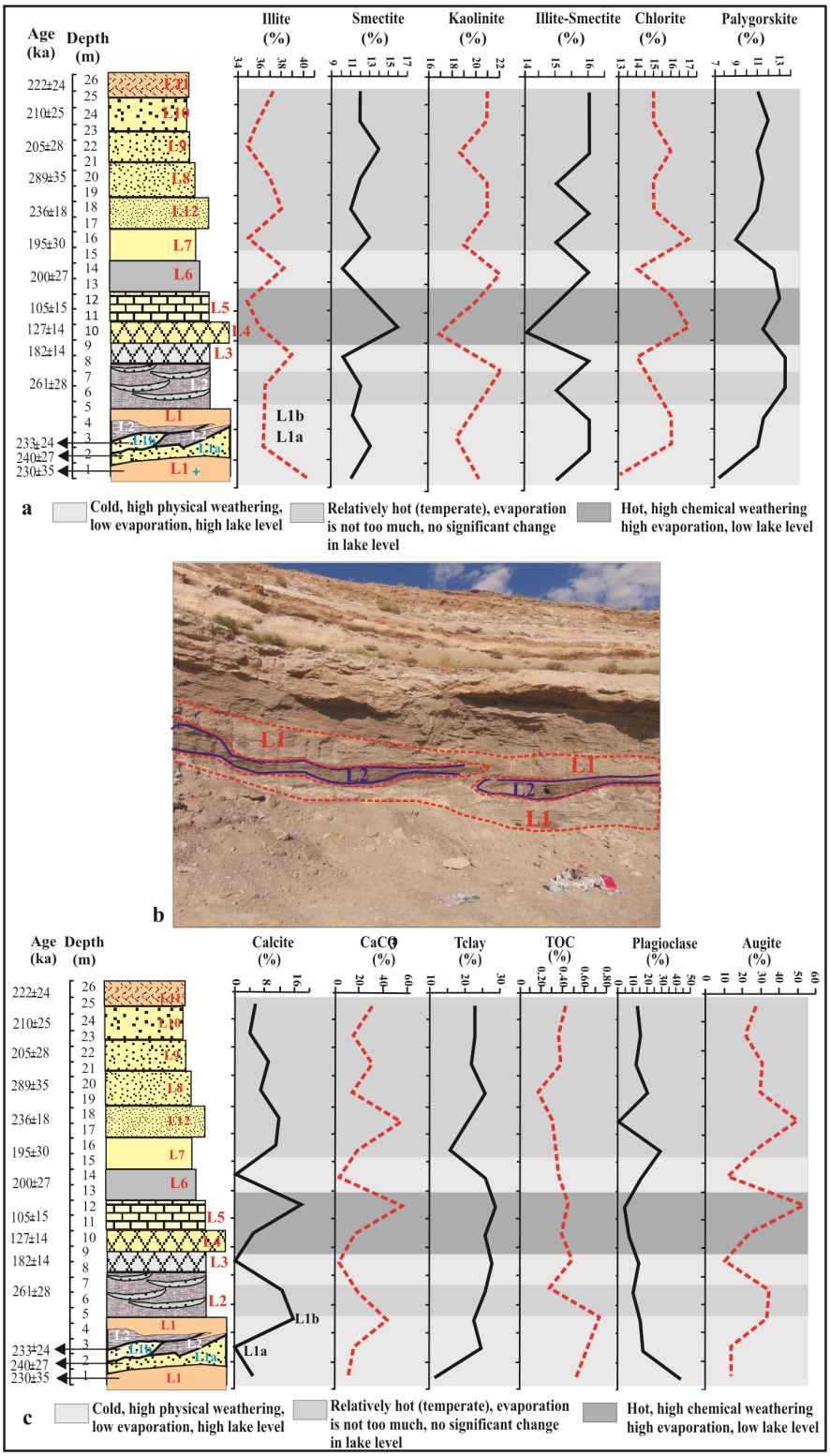

Fig. 9. a) Clay mineral content and chronological arrangement of deposition defined by delta and shoreline sediments accumulated in the environment of the old lake, b) L1 and L2 samples intermingled due to cross-bedding. During a period of heavy rain when flooding occurred, the L1 level was inserted into the L2 level and the layers were disordered, c) Mineral content, total clay (Tclay), total organic carbon (TOC), CaCO3 ratio, and OSL age of sequence defined by delta and shoreline deposition in an old lake environment.

augite in L2, L5, and L12 levels indicates that cinder cones surrounding the fan delta erupted. Also, the volcanic sand and gravel-sized material formed as a result of the volcanic activity of Leşkeri Hill mixed with this level (L8) during the period of development (transition from the Middle Pleistocene to the Late Pleistocene). Leşkeri Hill, which developed on the Lower Quaternary LFZ, is located north of the fan delta and is a monogenetic cone just south of Mt. Keçiboyduran. The streams that form the drainage in the volcanic products of Leşkeri Hill transported a large amount of volcanic origin material during the period when the L8 level developed (transition from the Middle Pleistocene to the Late Pleistocene). Augite derived from cinder cone (scoria cones) products was transported towards the lake by streams. Material from the north of the study area was certainly transported to the south and deposited. In addition, new sediment input was increased by the faulting that occurred in the period when the L7 level formed. New sediment input was also affected during the deposition of L7. Similarly, volcanic pebbles (basalt) forming the pebbly sandstone units at L9, L10, and L11 levels originated from activity in the surrounding volcanic mountains during the Late Pleistocene (Sönmez et al., 2018). In addition to clay minerals, TOC and $CaCO_3$ ratios were considered to interpret detritus minerals such as calcite, Tclay, and plagioclase in wet and arid conditions within the sequence of the fan delta (Fig. 9c). TOC and $CaCO_3$ availability rates can be indicators of climate change (Das et al., 2013).

5.2. Relationship between Quaternary global climate and ecological conditions

In this study, the OSL ages of sediment forming the fan delta were determined as the Marine Isotope Stages (MIS), MIS 6 (191-130 ka), MIS 5 (130-80 ka), and MIS 7 (243-191 ka) interglacial periods. There are more or fewer clay minerals at each level of lacustrine deposition (from L1 to L11) with more units from the MIS 7 period and a depth of approximately 30 m (Fig. 10). The investigation of spores and pollen in fan delta sediments is very important in terms of determining climate and vegetation changes in this period from the Pleistocene to the present day. In addition, palynological results, previously-mentioned OSL age results, and global climatic events are compatible. No abundant spores and/or pollen were found from the lowest to the middle of the sequence in the fan delta deposits due to clastic sediment deposition, and the paleo-vegetational results are added in the related section. Consequently, in this study, paleoclimatic interpretations were evaluated in the climatic process to which the samples belong.

The variety of pollen in the L7 sample is very low but the percentage is high. Pollen species belonging to herbaceous vegetation types of Amaranthaceae-Chenopodiaceae, *Daphne,* and Ranunculaceae-*Thalictrum* have high proportions in the sample, characterizing dry climatic conditions, and Asteraceae accompanies these pollen species with a low percentage. The L12 sample was precipitated at the end of the MIS 7e sub-phase. Although there were warm and dry climate conditions in this sub-phase, the climate changed to dry and cold in the MIS 7d sub-phase on a global scale. The abundance of Ranunculaceae-*Thalictrum* type, belonging to aquatic taxa, supports these climatic conditions in MIS 7d. At the end of the section in the Bor Plain (L11), the sedimentary sequences of the MIS 7d sub-phase were deposited in cold and dry climatic conditions. The high illite and low smectite ratios of the L11 sample match these climatic conditions (Fig. 10). Both deposition environments and/or volcanic activity had an impact on vegetation in the MIS 9a to MIS 5c phases. No pollen records were found from L6 to L11, as these conditions caused a reduction in vegetation due to fluvial conditions. Thus, sporomorph abundance was not found in the

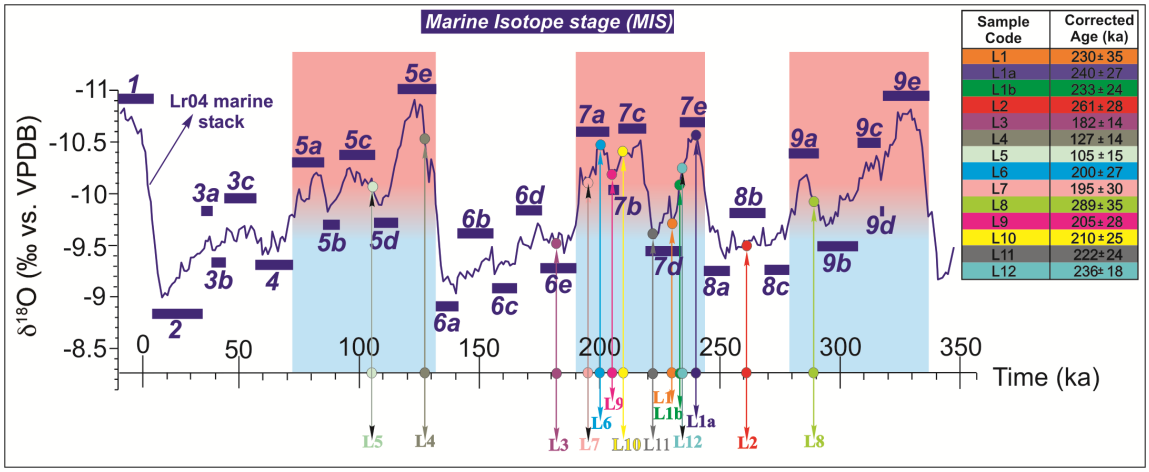

Fig. 10. Location of samples in MIS period.

lower levels of the fan delta due to flooding of water and washing. Studies about paleoclimate using pollen diagrams indicate that lacustrine sediments with aquatic and meadow plants such as Ranunculaceae-*Thalictrum* were deposited during a temperate climate in Turkey and Europe (Caspers and Freund, 2001; Nuvenko and Zuganova, 2010; Demirer et al., 2016). Amaranthaceae-Chenopodiaceae has a high percentage in the L7 sample, characterizing dry climatic conditions (Kayseri-Özer and Emre, 2022). According to Freitag et al. (1999), the existence of Chenopodiaceae supports a dry environment and might have invaded Central Anatolia later during the drier climatic phases of the Pleistocene. *Artemisia* (Asteraceae) pollen decreases and Chenopodiaceae increases with increasing aridity (Alçiçek et al., 2017); the ratio of their pollen is used as a moisture indicator. This condition is evident in L7. Increases in Chenopodiaceae pollen with the amount of *Artemisia* indicate intense aridity during the late glacial times (El-Moslimany, 1990).

6. CONCLUSIONS

The fan delta deposition system is on the fault-controlled foothill of Mt. Keçiboyduran, bordering the southwest of the Bor Plain. Tectonism, volcanism, and paleoclimate that developed in different periods controlled the lithofacies features. Furthermore, travertine or tufa-type carbonates must have formed as a product of groundwater evaporation, where precipitation was interrupted during dry periods. The volcanic activity of the Leşkeri monogenic volcanic mass reactivated during the transition from the Middle to Late Pleistocene—the deposition time of the L8 (MIS 9a), L9 (MIS 7b), and L10 (MIS 7c) samples. The Pleistocene activity of Leşkeri Hill was observed to affect sedimentation after volcanic activity, and gravelly sandstone units and volcanic pebbles (basalt) were deposited at this level. The abundance of volcanic material in the sediments indicates that the Quaternary monogenic ash cones in the immediate vicinity affected regression and dried the lake. Thus, volcanic, and tectonic processes and climate caused fluctuations in the lake level. Drainage developing between the monogenic volcanic cones in the Middle Pleistocene caused the accumulation of sediments in the lake and the formation of a deltaic fan environment. The retreat lasted with uncertain oscillations until the late Holocene. The lowest shoreline system corresponding to the Upper Pleistocene is between 1100 m and 1110 m (asl). These elevations are also the level where the lake terraces are located, and the lake level reaches approximately 60 to 40 m above the lake floor. After this phase, the lake retreated significantly in the Late Pleistocene-Early Holocene. The paleoenvironmental conditions are supported by the presence of herbaceous species (Asteraceae–*Asteroidea* type, *Daphne*, and Ranunculaceae–*Thalictrum*), indicating relatively a high percentage of temperate climate conditions at the upper levels. The small-scale, high-frequency changes in the fan delta sequence and inferred lake-level fluctuations must have been controlled by short-term climatic changes in MIS 7. Herbaceous vegetation pollen, such as Amaranthaceae–Chenopodiaceae, *Daphne*, and Asteraceae, support warm and dry climatic conditions during climatic phases causing the lake's retreat and high evaporation. Furthermore, the abundant recording of the Ranunculaceae–*Thalictrum* herbaceous vegetation growing at the water's edge and in meadows during development stages could be related to the humid phase in climatic conditions. However, during the Pleistocene period, no dense arboreal paleovegetation formed forests in the basin because only nonarboreal plants (herb species) were identified in the samples from Bor Plain. Thus, steppe vegetation dominated around the lake because of the effect of a locally changing climate during this period.

Peer Review: Externally peer-reviewed.
Author Contributions: Conception/Design of Study- T.B.A., B.N.A., Z.S.K., M.S.K.Ö.; Data Acquisition- T.B.A., B.N.A., Z.S.K., M.S.K.Ö.; Data Analysis/Interpretation- T.B.A., B.N.A., Z.S.K., M.S.K.Ö.; Drafting Manuscript- T.B.A.; Critical Revision of Manuscript- B.N.A., Z.S.K., M.S.K.Ö.; Final Approval and Accountability- T.B.A., B.N.A., Z.S.K., M.S.K.Ö.
Conflict of Interest: Authors declared no conflict of interest.
Financial Disclosure: This research was funded by the TÜBİTAK (Project no. 116Y498).
Acknowledgment: This research was funded by the TÜBİTAK (Project no. 116Y498). We are grateful to Yavuz Sürme (Niğde Ömer Halisdemir University) for his technical support in the laboratory, Serkan Kükrer (Ardahan University) for TOC analyses, and Eren Şahiner and Niyazi Meriç for OSL dating (Ankara University Institute of Nuclear Sciences).

REFERENCES

Agostini, S., Manetti, P., Lustrino, M., Di Giuseppe P., Savaşçın, MY., Ersoy, Y., Karaoğlu, Ö. (2015). Central and Eastern Anatolia Volcanism. In: Agostini, S., Manetti, P., Lustrino, M. (Eds.), The Contribution of Italian Scientists to the Geology of the Turkey. *Acta Vulcanologica, 26-27*, 37-50.

Akıska, E., Varol, B. (2020). Alluvial-lacustrine sedimentation and volcaniclastic deposition in an intracontinental tectonic graben: paleoenvironmental evolution of the Neogene Sinanpaşa Basin, west-central Turkey. *Turkish Journal Earth Science, 29*, 295-324.

Alçiçek, H., Varol, B., Özkul, M. (2007). Sedimentary facies, depositional environment sand paleogeographic evolution of the Neogene Denizli Basin of SW Anatolia, Turkey. *Sedimentary Geology, 20*, 596-637.

Alçiçek, H., Wesselingh, FP., Alçiçek, MC., Jimenez-Moreno, G., Feijen, FJ., Ostende, van den H., Mayda, S., Tesakov AS. (2017). A multiproxy study of the early Pleistocene palaeoenvironmental and palaeoclimatic conditions of an anastomosed fluvial sequence from the Çameli Basin (SW Anatolia, Turkey). *Palaeogeography, Palaeoclimatology, Palaeoecology, 467*, 232–252.

Atabey, E., Göncüoğlu, CM., Turhan, N. (1990). 1/100,000 Scale Geology Map, Kozan-J19 section of the map. Publication of General Directorate of Mineral Research and Exploration.

Bayer-Altın, T., El Quahabi, M., Fagel, N. (2015). Environmental and climatic changes during the Pleistocene-Holocene in the Bor Plain, Central Anatolia, Turkey. *Palaeogeography, Palaeoclimatology, Palaeoecology, 440*, 564-578.

Bayer-Altın, T., Kayseri-Özer, MS., Altın, BN. (2021). The Holocene terraces of the desiccated Bor Lake and Neolithic occupation in Bor Plain, Central Anatolia, Turkey. *Environmental Earth Sciences, 80*, 1-27.

Beekman, PH. (1966). The Pliocene and Quaternary volcanism in the Hasan Dağ-Melendiz Dağ region. *Bulletin of the Mineral Research and Exploration, 66*, 88-103.

Beug, HJ. (2004). *Leitfaden der Pollenbestimmung für Mitteleuropa und angrenzende Gebite*. Verlag Friedrich Pfeil, Munich, 542 pp (in German).

Boggs, SJr. (2009). Petrology of sedimentary rocks. In Boggs SJr (Ed.), *Carbonate sedimentary rocks* (pp. 311-408). Cambridge, Cambridge University Press.

Caspers, G., Freund, H. (2001). Vegetation and climate in the Early- and Pleni-Weichselian in northern Central Europe. *Journal of Quaternary Science, 16*, 31-48.

Cohen, H., Erol, O. (1969). Aspects of the palaeogeography of Central Anatolia. *The Geographical Journal, 135*, 388-398.

Colella, A., Prior, DB., Mccabe, A. (1992). Coarse-grained deltas (Special publication no 10 of the international association of sedimentologists). *Journal of Quaternary Science, 7*, 271-272.

Collinson, JD. (1996). Alluvial sediments. In Reading, HG. (Ed.), *Sedimentary environments: processes, facies and stratigraphy* (pp. 37-81). Oxford, Blackwell Science.

Cook, HE., Johnson, PD., Matti, JC., Zemmels, I. (1975). *IV. Methods of sample preparation, and Xray diffraction data analysis, X-ray mineralogy laboratory, Deep Sea Drilling Project, University of California, Riverside*. Initial Reports of the Deep Sea Drilling Project, 25, U.S. Govt. Washington, Printing Office.

Cramer, MD., Hawkins, HJ. (2009). A physiological mechanism for the formation of root casts. *Palaeogeography, Palaeoclimatology, Palaeoecology, 274*, 125-133.

Das, SS., Rai, AK., Akaram, V., Verma, D., Pandey, AC., Dutta, K., Prasad, RGV. (2013). Paleoenvironmental significance of clay mineral assemblages in the southeastern Arabian Sea during last 30 kyr. *Journal of Earth System Science, 122*, 173-185.

De Celles, PG., Gray, MB., Ridgway, KD. Cole, RB., Pivnik, DA., Pequera, N., Srivastava, P. (1991). Controls on synorogenic alluvial-fan architecture, Beartooth Conglomerate (Palaeocene), *Wyoming and Montana. Sedimentology, 38*, 567-590.

Demirer, ŞS., Akgün, F., Tunoğlu, C., Tuncer, A., Kayseri-Özer, MS. (2016). Pliocene vegetation and climate reconstruction based on pollen data from Dombayova Graben (Afyonkarahisar, Western Anatolia). 17. Paleontology - Stratigraphy Workshop, Balıkesir, Türkiye.

Doğan-Külahçı, GD., Temel, A., Gourgaud, A., Varol, E., Guillou, H., Deniel, C. (2018). Contemporaneous alkaline and calc-alkaline series in Central Anatolia (Turkey): Spatio-temporal evolution of a post-collisional Quaternary basaltic volcanism. *Journal of Volcanology and Geothermal Research, 156*, 56-74.

El-Moslimany, PA. (1990). Ecological significance of common nonarboreal pollen: examples from drylands of the Middle East. *Review of Palaeobotany and Palynology, 64*, 343-350.

Emre, Ö. (1991). *Hasanağı-Keçiboyduran Dağı yöresi volkanizmasının jeomorfolojisi (Geomorphology of the volcanism of Mt. Hasan-Mt. Keçiboyduran)* (Doktora Tezi). Institute of Social Sciences, Istanbul University, İstanbul.

Erol, O. (1991). The relationship between the phases of the development of the Konya-Karapinar obruks and the Pleistocene Tuz Gölü and Konya pluvial lakes, Turkey. *Deniz Bilimleri ve Coğrafya Enstitüsü Bülteni, 7*, 5-49 (in Turkish with English abstract).

Freitag, H., Vural, M., Adıgüzel, N. (1999). A remarkable new *Salsola* and some new records of *Chenopodiaceae* from Central Anatolia, Turkey. *Willdenowia, 29*, 123-139.

Gaudette, HE., Flight, WR., Toner, L., Folger, DW. (1974). An inexpensive titration method for the determination of organic carbon in recent sediments. *Journal of Sedimentary Research,* 44, 249-253.

Göncüoğlu, M., Dirik, K., Erler, A., Yalınız, K., Özgül, K., Çemen, İ. (1996). *Tuzgölü havzası batı kısmının temel jeolojik sorunları (Basic Geologic Problems of Western Part of Tuzgölü Basin).* Turkish Petroleum Corporation (TPAO) Report, 3753.

Göz, E., Kadiri, S., Gürel, A., Eren, M. (2014). Geology, mineralogy, geochemistry, and depositional environment of a Late Miocene/ Pliocene fluvio-lacustrine succession, Cappadocian Volcanic Province, central Anatolia, Turkey. *Turkish Journal of Earth Science, 23*, 386-411.

Gradusov, BP. (1974). A tentative study of clay mineral distribution in soils of the World. *Geoderma, 12*, 49-55.

Grant, WH. (1963). Weathering of Stone Mountain granite. *Clays and Clay Minerals, 11*, 65-73.

Gruszka, B., Zieliński, T. (2021). Lacustrine deltas and subaqueous fans: almost the same, but different – a review. *Geologos, 27*, 43-55.

Gürel, A., Lermi, A. (2008). Geo-archaeological activities in southern Cappadocia, Turkey. In D'Alfonso, L., Balza, ME., Mora, C. (Eds.), *Studia Mediterranea* (pp. 55-68). Pavia: Italian University Press.

Hadji, F., Marok, A., Mokhtar Samet, A. (2019). Miocene sediment mineralogy of the lower Chelif basin (NW Algeria): implications for weathering and provenance. *Turkish Journal of Earth Sciences, 28*, 85-102.

Hardie, LA., Smoot, JP., Eugster, HP. (1978). Saline lake sand their deposits: a sedimentological approach. In Matter, A., Tucker, M.E. (Eds.), *Modern and ancient lake sediments* (pp. 7-41). Ghent: Special Publications of the International Association of Sedimentologists.

Horton, BK., Schmitt, JG. (1996). Sedimentology of a lacustrine fan delta system Miocene Horse Camp Formation. *Sedimentology, 43*, 133-155.

Ilgar, A., Nemec, W. (2005). Early Miocene lacustrine deposits and sequence stratigraphy of the Ermenek Basin, Central Taurides, Turkey. *Sedimentary Geology, 173*, 233-275.

Karabıyıkoğlu, M., Kuzucuoğlu, C., Fontugne, M. (1999). Facies and depositional sequences of the Late Pleistocene Göçü shoreline system, Konya basin, Central Anatolia: Implications for reconstructing lake-level changes. *Quaternary Science Reviews, 18,* 593-609.

Karabıyıkoğlu, M. (2003). Konya Havzasının Geç Kuvaterner evrimi (The Late Quaternary evolution of the Konya Basin) (Doktora Tezi), İstanbul Üniversitesi Sosyal Bilimler Enstitüsü, İstanbul.

Kayseri-Özer, MS., Emre, T. (2022). Palynology and Palaeoclimate of the coal-bearing sediments in north Aydın-Köşk (Büyük Menderes Graben). *Review of Paleobotany and Palynology, 297*, 104560.

Kuzucuoglu, C. (2019). Geomorphological landscapes in the Konya Plain and surroundings, In Kuzucuoğlu C, Çiner A, Kazancı N. (Eds.) *Landscapes and Landforms of Turkey* (pp. 353-368). Berlin: Springer.

Kuzucuoğlu, C., Gündoğdu-Atakay, E., Mouralis, D., Atıcı, G., Guillou, H., Türkecan, A., Pastre, J-F. (2020). Geomorphology and tephrochronoglogy in the Hasandağ volcano (southern Cappadocia, Turkey). *Mediterranean Geoscience Review, 2*, 185-215.

Moore, MD., Reynolds, CR. (1997). X-ray Diffraction and Identification and Analysis of Clay Minerals. Oxford: Oxford University Press.

Nesbitt, HW., Young, GM., McLennan, SM., Keays, RR. (1996). Effects of chemical weathering and sorting on the petrogenesis of siliciclastic sediments, with Implications for provenance studies. *The Journal of Geology, 104*, 525-542.

Nuvenko, EY., Zuganova, IS. (2010). Landscape dynamics in the Eemian interglacial and Early Weichselian Glacial Epoch on the South Valdai Hills (Russia). *The Open Geography Journal, 3*, 44-54.

Orton, GJ., Reading, HG. (1993). Variability of deltic processes in terms of sediments supply, with particular emphasis on grain size. *Sedimentology, 40*, 475-512.

Roberts, N. (1983). Age, palaeoenvironments and climatic significance of Late Pleistocene Konya lake, Turkey. *Quaternary Research, 19*, 154-171.

Rodriguez, AB., Hamilton, MD., Anderson, JB. (2000). Facies and evolution of the modern Brazos Delta, Texas: wave versus flood influence. *Journal of Sedimentary Research, 70*, 283-295.

Rust, BR. (1978). Depositional models for braided alluvium. Canadian Society of Petroleum *Geologists Memoirs, 5*, 605-625.

Smith, GA. (1986). Coarse-grainned nonmarine volcano clastic sediment: terminology and depositional process. *Geological Society of America Bulletin, 97*, 759-772.

Sönmez, M., Aydın, F., Lermi, A., Saka, SO. (2018). The geology and volcano stratigraphy of western part of Niğde volcanic complex (Cappadocia, Central Anatolia): mount Keçiboyduran and its near surroundings. *Niğde Ömer Halisdemir University Journal of Engineering Sciences, Special Issue, 3*, 1170-1174.

Tekin, E., Varol, B., Ayyildiz, T., Karakaş, Z. (2005). Polatlı Havzası (İç Anadolu) Kırıntılı Kuvaterner çökellerinde otijenik manganokalsit-(Ca.Mn)CO_3 oluşumu (Autigenic manganocalcite-(Ca.Mn)CO_3 in the declastic Quaternary sediments of the Polatlı Basin, Central Anatolia)(pp. 136-135). 17th National Congress of Electron Microscopy, Kocaeli, Türkiye.

Ulu, Ü. (2009). 1/100.000 Scale Geology Map, Karaman-M32 section of the map. General Directorate of Mineral Research and Exploration, Report No. 127.

Varol, B., Şen, Ş., Ayyıldız, T., Sözeri, K., Karakaş, Z., Metais, G. (2016). Sedimentology and stratigraphy of Cenozoicdeposits in the Kağızman-Tuzluca Basin, northeastern Turkey. *International Journal of Earth Sciences, 105*, 107-137.

Weaver, CE. (1989). *Clays, muds, and shales*. Amsterdam: Elsevier.

Woronko, B., Pochocka-Szwarc, K. (2013). Depositional environment of a fan delta in a Vistulian proglacial lake (Skaliska Basin, north-eastern Poland). *Acta Palaeobotanica,* 53, 9-21.